Chapter 5

Discussion

5.1 The effects of the difference of Al_2O_3 powder for density and microstructure

In this experiment, AKP-30 and AES-11 alumina powder were used as raw materials. The powders have high purity and fine average particle size less than 1 μm as shown in Table 3.1. AKP-30 and AES-11 alumina powder can be sintered to nearly theoretical density as shown in Fig.4.3(a) and (b), at 1600-1650 ^{o}C. On the other hand, at lower temperature as 1450 – 1500 ^{o}C, most specimens of AKP-30 showed higher density than AES-11. Especially, specimens of 2.1 and 2.2 composition reached almost full density even sintered at 1450 and 1500 ^{o}C. This difference was thought to be due to the particle size and shape as shown in Fig.4.1 and Fig.4.2, respectively. AES-11 specimens have finer-grained microstructure than that of AKP-30, as shown in Table 4.2. The grain size of composition 2.1 – 2.4 (AKP-30 with no additives, 0.5%MgO, 1.5%, 3.0%ZrO_2) were rather big comparing to other compositions. ZrO_2 addition of 7.5 wt% (5.0vol%) inhibited grain growth. From Fig.4.7, it is obvious that the grains AKP-30 easily grew when there is no much amount of grain growth inhibitor.

The thermal conductivity of composition used AKP-30 are, in average, higher than that of AES-11. Relative densities of specimens of either Al_2O_3 are similar as seen in Table 4.1. Consequently, the reason why specimen made of AKP-30 show higher thermal conductivity is still unknown.

5.2 The effects of the difference of additives for density and microstructure

MgO and ZrO_2 were used as additives in this experiment. MgO doped compositions can be sintered to almost full density at 1600-1650 ^{o}C, as shown in Fig.4.3 (a) and (b). The effect of MgO is due to the elimination of discontinuous grain growth during the late stages of sintering. Therefore MgO also affects to decrease the average grain size of AKP-30 and AES-11 as shown in Table 4.2. Microstructures of doped MgO compositions exhibit equiaxial grain shape as shown in Appendix 7.

Most of ZrO_2 particles were located at 3- and 4-grain junctions of alumina grain, as shown in Appendix 7. The particles exerted a dragging force at the grain junctions to limit grain growth. Therefore, at low temperature as 1450 – 1500 ^{o}C, ZrO_2 doped specimens 2.3 – 2.5 showed lower relative density. However, at higher temperature, motive force to sinter alumina was larger than the grain growth inhibition effect of ZrO_2 particles, as shown in Fig.4.2(a). Grain growth control was achieved when a majority or all 3- and 4-grain junctions contained a ZrO_2 inclusion. For doped compositions, the grain size was inversely proportional to the volume fraction of ZrO_2 as shown in Fig.4.6. Microstructures of doped compositions exhibit equiaxial grain shape.

5.3 The cause of deviation in relative density

As seen in Fig.4.2(a), the relationships between relative density and sintering temperature were very smooth for compositions 2.3 – 2.5. On the other hand, the relationships for 2.1 – 2.2 were not natural. The relationships for compositions 2.6 – 2.10 (Fig.4.2(b)) were also not natural nor smooth. Same unnatural tendency were also seen in Fig.4.8.

In Appendix 6, the deviation among 3 specimens for each composition was small. In Appendix 8, the deviations among 5 specimens for each composition were in most cases less than 3%, sometimes 3 - 5% as shown in Fig.5.1. In this experiment, the diameter of specimens were 35 mm. In Appendix 13, relative densities of each 3 specimens for 15 cases, which are different in compositions, soaking time and sintering temperature, are shown. In most cases, the deviation was less than 3%, however, the deviation was more than 3% in 8 cases and maximum was 14.8%.

Then the cause of deviation was analyzed. One cause was come from the lack of drying, as seen in Fig.5.1. In this experiment, specimens were dried for 30 min in an oven at 100 – 105 ^{o}C. The time was not enough for specimens with high water absorption. As seen in Fig.5.1, specimens with low water absorption (Fig.4.10), were sintered at 1550 – 1650 ^{o}C, showed also deviation over 3%. In this case, saturated weight was heavier than dry weight in most measurement. In Appendix 4 and Appendix 13, the differences were not so much as in Appendix 8. There was some problem in the water wiping process in the experiment of Appendix 8. From above discussion, relative densities at 1550 – 1650 ^{o}C in Fig.4.9 might be 2 – 3 % higher than the data. Comparing Fig.4.3(b) and Fig.4.9, the deviation of relative density between compositions 2.6 – 2.10 are small in Fig.4.9. On the other hand, the deviation is large in Fig.4.3(b). The reason of this difference could not be explained from the measurement data.

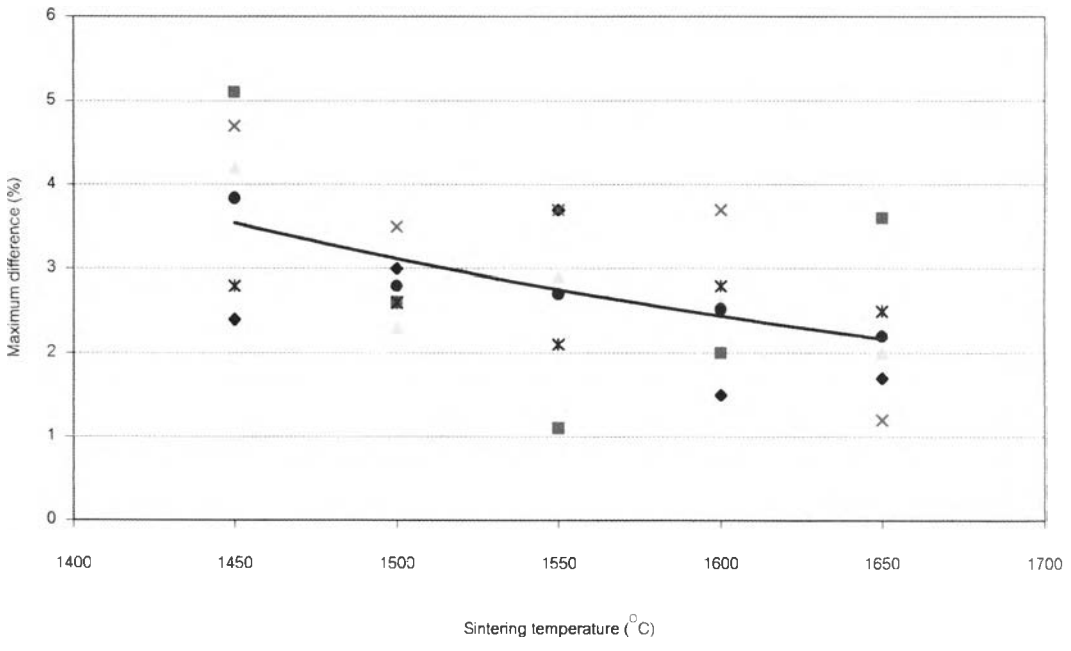

Fig.5.1 The relationship between sintering temperature and maximum difference (%).

Another possibility of deviation is the sintering process. Specimens were set on a setter. If there was temperature difference in the area of setter, density difference between specimens should be occurred. In Appendix 13, however, more than 20 sets of specimens showed less than 1 % deviation in each sintering condition. In this case the heat accumulation in a setter was minimum.

One more cause of deviation may be the deviation of pressed density, In this experiment, specimen was only pressed by axial press, not isostatic press. The pressure gauge of the press machine was not so accurate. So, there must be some difference of green density in these specimens. In this case, CIP method (Cold Isostatic Pressing) will be suggested for future experiment.

In the measurement of thermal conductivity (κ), thermal diffusivity (θ) is measured directly. And κ is the product of θ times bulk density (d). Therefore, if d is not correct, κ is not correct. As discussed above, there are some deviation in thickness d in this experiment. To assure the accurate of κ values, the thickness d for all specimens, were remeasured. All data are shown in Appendix 17. And the standard deviation of the two measurement was 0.31% for AKP-30 specimens and 0.088% for AES-11 specimens. Consequently, the d of specimen supplied to measure κ was correct.

Fig.5.2 shows the correlation between first and second measurement data for mixed additives. Original data are filed in Appendix 16. Most of the data are in the range of ±2%. These differences were come from some difference in measurement techniques and human error in measurement using Archimedes' method.

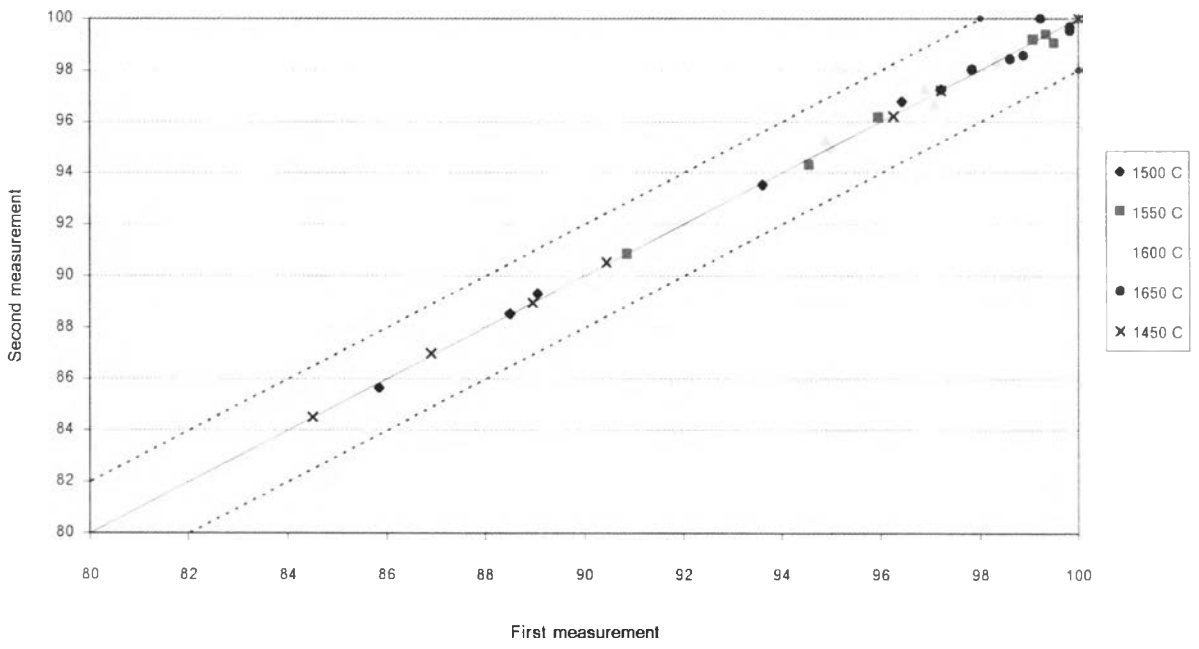

(a) No.1 specimen, 1450 – 1650 ^{O}C

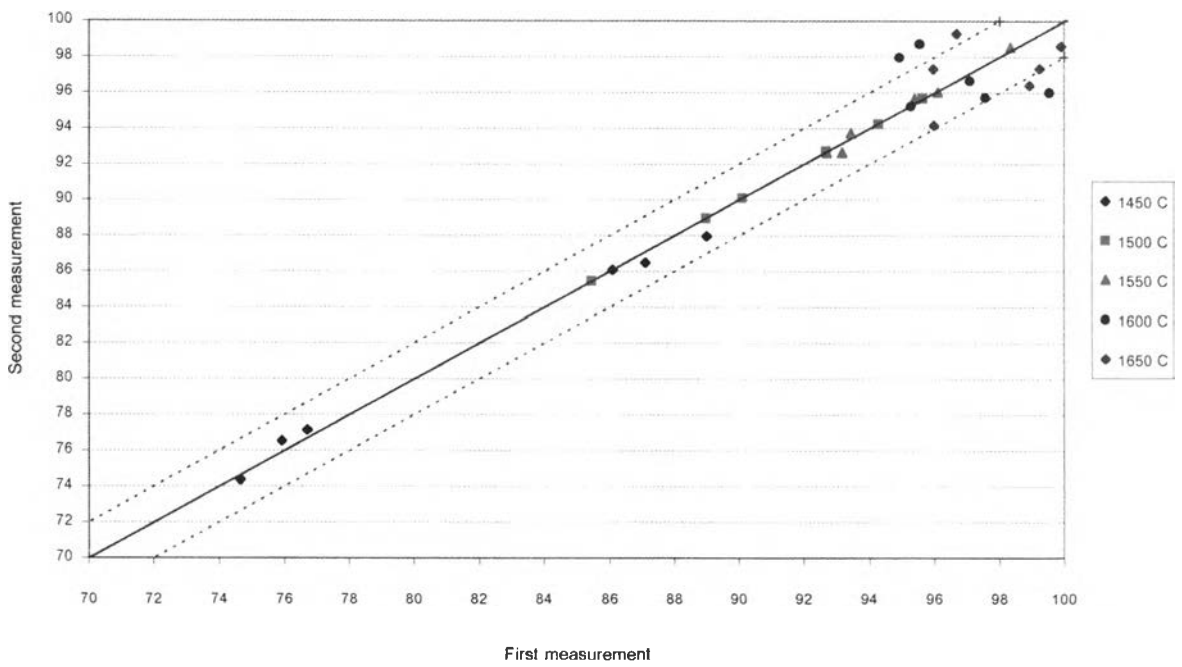

(b) No.2 specimen, 1450 – 1650 ^{O}C

Fig.5.2 The relationship of the relative density between the repeated measurement for specimen No.1 and specimen No.2

5.4 Mechanical strength

As seen in Fig.4.8, mechanical strength of specimens sintered at 1600 ^{o}C were higher than that at 1650 ^{o}C. Relative densities of specimens sintered at 1600 ^{o}C were similar or a little lower than that at 1650 ^{o}C, as seen in Fig.4.9. SEM photographs of specimen 2.7 (MgO 0.5%) and 2.8 (ZrO_2 1.5%) sintered at 1600 ^{o}C are shown in Fig.5.3 and Fig.5.4. Comparing Fig.5.3 and Fig.5.4 with SEM photographs of same compositions in Appendix 7, the grain sizes of specimens sintered at 1600 ^{o}C were obviously smaller than that at 1650 ^{o}C. Therefore, it is concluded that the highest strength of specimens sintered at 1600 ^{o}C are due to the fine grain sizes.

The mechanical strength was measured in conformity with ASTM. The maximum value of 500 – 600 Mpa was shown in Fig.4.8, are rather too high for typical alumina ceramics. The contact area used for calculating mechanical strength was a radius of ram tip which the radius of a ram tip was used as a contact area for calculating mechanical strength in this study as shown in Appendix 3 part 4. Using the contact area as the radius B may affect the degree of accuracy values. The relationship between strength and the diameter of radius tip should be confirmed in future experiment.

The surface roughness profile of specimens are shown in Appendix 12. The surface roughness profile of the substrate, which AISIN currently uses, is shown in 5.5(a) and (b). The profiles are significantly different. The sample preparation procedures prior to the measurement of AISIN and our samples are different. The surface of our specimens were ground and polished but the surface of AISIN samples were ground and no evidence of polishing. One of our objective is to get strong enough material compared to AISIN substrate. In this study, our samples showed high mechanical strength but can not compare with AISIN substrate. This is due to the differences in thickness and surface condition. AISIN sample was prepared with very thin thickness and the surface condition was different as well.

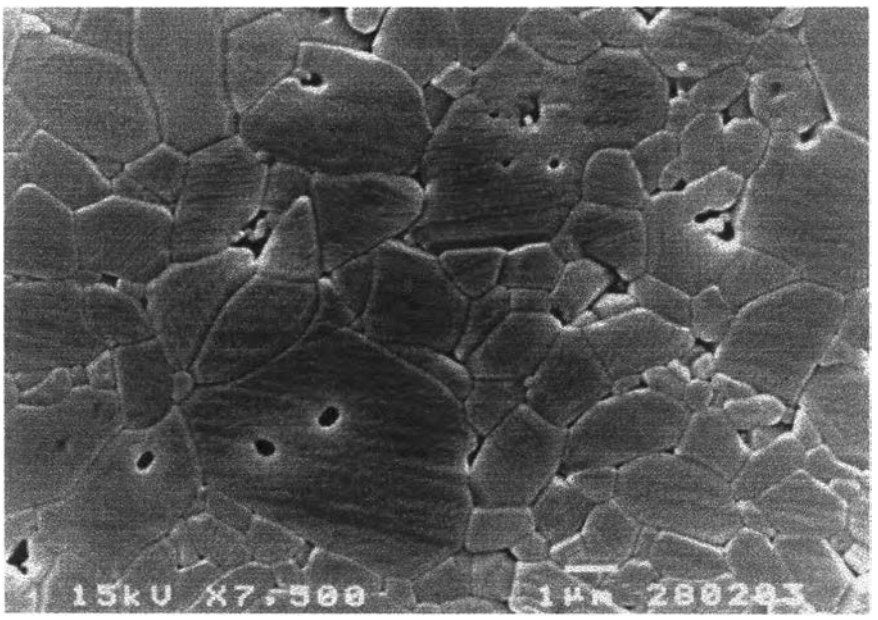

Fig.5.3 SEM Micrograph of 0.5%MgO doped AES-11 alumina sintered at 1600 ^{O}C 2 h.

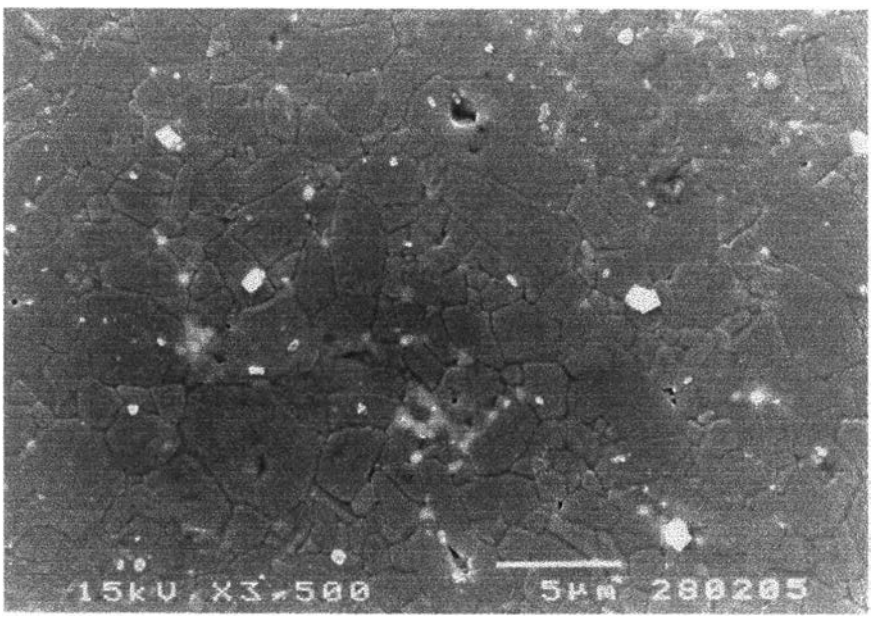

Fig.5.4 SEM Micrograph of 1.5%ZrO_2 doped AES-11 alumina sintered at 1600 ^{O}C 2 h.

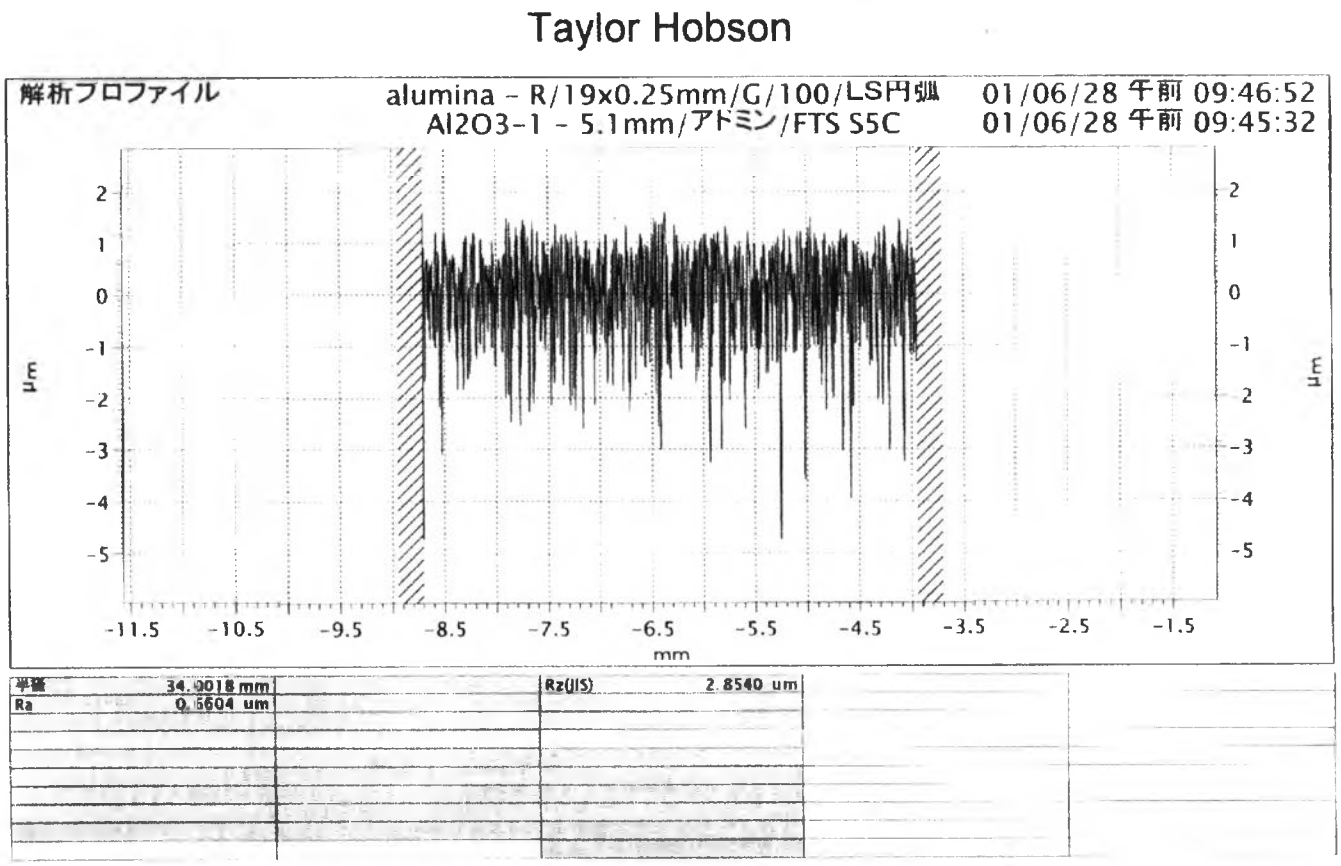

Fig.5.5(a) Surface roughness of alumina of AISIN.

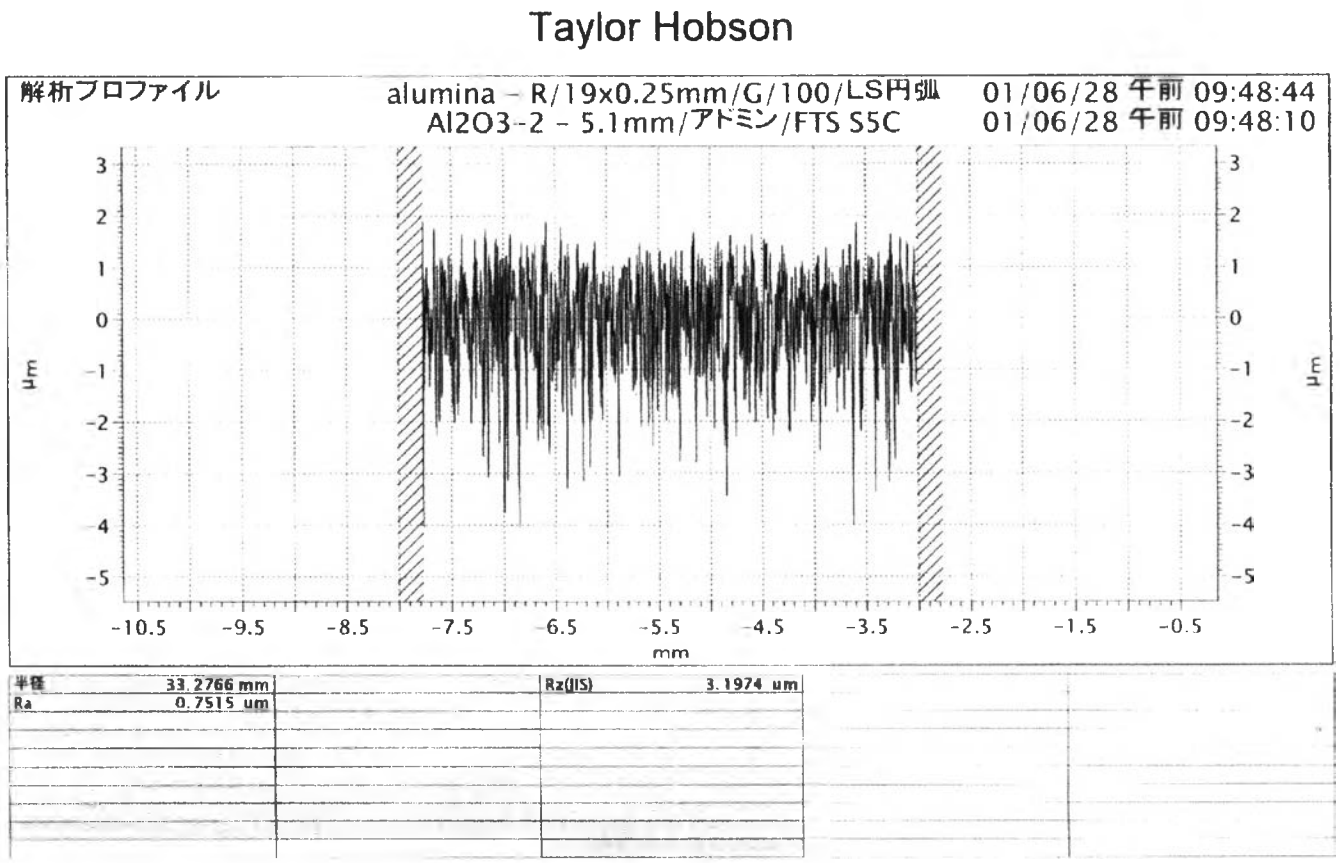

Fig.5.5(b) Surface roughness of alumina of AISIN.

5.5 Thermal conductivity

The mechanical strength of specimens sintered at 1600 ^{o}C was high. So, thermal conductivity of some of the specimens were measured in addition. All data including the data in Table 4.1 are shown in Table 5.1.

The thermal conductivity of a composite depends on the microstructure. When a second phase disperses in a matrix, the thermal conductivity of the composite (κ_m) is shown by the following equation[2.32].

$$\kappa_m = \kappa_c \cdot \frac{1+2\nu_d(1-\kappa_c/\kappa_d)/(2\kappa_c/\kappa_d+1)}{1-\nu_d(1-\kappa_c/\kappa_d)/(\kappa_c/\kappa_d+1)} \qquad (5.1)$$

κ_c is the thermal conductivity of matrix, κ_d is the thermal conductivity of dispersed phase, and ν_d is the volume fraction of dispersed phase. When $\kappa_c >> \kappa_d$, following equation is derived.

$$\kappa_m \approx \kappa_c [(1-\nu_d)/(1+\nu_d)] \qquad (5.2)$$

In this experiment, ZrO_2 and pore are the second phase. The thermal conductivity of ZrO_2, 3 W/m·K, is lower than that of Al_2O_3, 40 W/m·K. Then, we can apply equation 5.2 to our experimental results. The volume of ν_d is the sum of pore volume and ZrO_2 volume. From the relative density and ZrO_2 content, ν_d was calculated. All data used to calculate equation 5.2 and the result κ_m are shown in Table 5.1.

Table 5.1 Measured thermal conductivity and calculated thermal conductivity based on equation(5.2)

Composition		Measurement thermal conductivity (W/m·K)	Relative density	1-Relative density	Volume of ZrO_2	v_d	K_m (W/m·K)
AKP-30 1650°C	2-1.	35.5	0.97	0.03	0.00	0.03	37.7
	2-2.	37.2	0.98	0.02	0.00	0.02	38.4
	2-3.	34.1	0.95	0.05	0.01	0.06	35.5
	2-4.	30.8	0.97	0.03	0.02	0.05	36.2
	2-5.	30.1	0.96	0.04	0.05	0.09	33.4
AES-11 1650°C	2-6.	31.8	0.96	0.04	0.00	0.04	36.9
	2-7.	30.8	0.96	0.04	0.00	0.04	36.9
	2-8.	31.4	0.98	0.02	0.01	0.03	37.7
	2-9.	33.5	0.98	0.02	0.02	0.04	36.9
	2-10.	29.8	0.98	0.02	0.05	0.07	34.8
AES-11 1600°C	2-6.	27.2	0.94	0.06	0.00	0.06	35.5
	2-7.	30.4	0.97	0.03	0.00	0.03	37.7
	2-8.	31.3	0.97	0.03	0.01	0.04	36.9
	2-9.	30.5	0.96	0.04	0.02	0.06	35.5
Y-A995		24.3	0.89	0.11	0.00	0.11	32.1
#AISIN		24.0	0.95	0.05	0.06	0.11	32.1

#The purity of Al_2O_3 is 96.55%. Other compositions are SiO_2 2.22, MgO 0.96, CaO 0.17, NaO 0.05, Fe_2O_3 0.03, CuO 0.02, K_2O <0.01 (%). Assume that these additives make glass of 2.2 g/cm^3 in grain boundaries, true density of AISIN substrate is 3.91 g/cm^3 and the volume of v_d except pore is about 0.06. The specific density measured is 3.70 g/cm^3. So, relative density 3.70/3.91 = 0.95.

All thermal conductivity data related to relative density and ZrO_2 content are shown in Fig.5.5 and Fig.5.6. Obviously, Fig.5.5 and Fig.5.6 have not good relationship between the thermal conductivity and those properties.

Fig.5.7 shows the relationship between κ_m and measured thermal conductivity. When pores and ZrO_2 grains are dispersed in the alumina matrix like the model for equation (5.2), measured thermal conductivity and κ_m should be equal. Then, the data should be plotted on the 1=1 line in Fig.5.7. However, measured values are always a little smaller than that of κ_m, as seen in Fig.5.7. The difference between κ_m and measured value becomes large when κ_m becomes small. The κ_m of AISIN substrate was calculated on the assumption explained under Table 5.1. Measured value and κ_m for Y-A995 and AISIN were almost same by just a coinsidence. The cause of the difference for AISIN substrate will come from the gap between grains as seen in Fig.5.8. The microstructure of Y-A995 is shown in Fig.5.9. There are some narrow gap between Al_2O_3 grains. These gap must be the cause of the difference from the κ_m. Comparing data for specimens made of AKP-30 and AES-11, measured data of AKP-30 are close to κ_m.

Measured thermal conductivity are over 30 W/m•k except 2-10 (AES-11, 1650 ^{o}C) and 2-6 (AES-11, 1600 ^{o}C). Obviously, 7.5 wt% ZrO_2 decreases the thermal conductivity. It is expected that when κ_m is over 35 W/m•K, the measured thermal conductivity will be over 30 W/m•K.

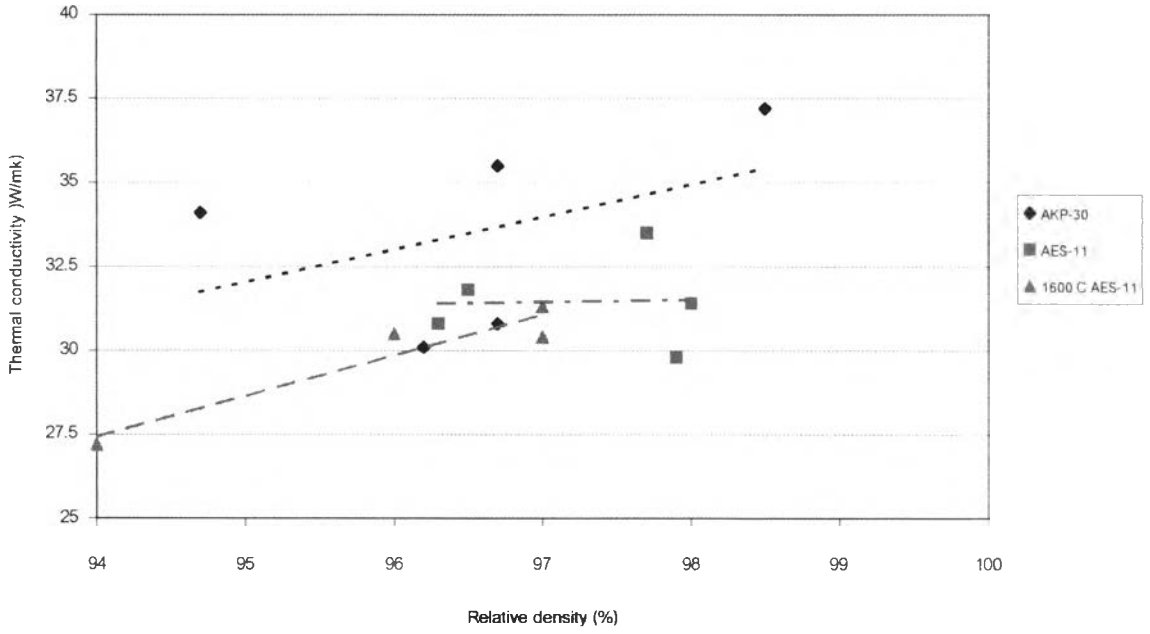

Fig.5.6 Relationship between relative density and thermal conductivity of AKP-30 and AES-11.

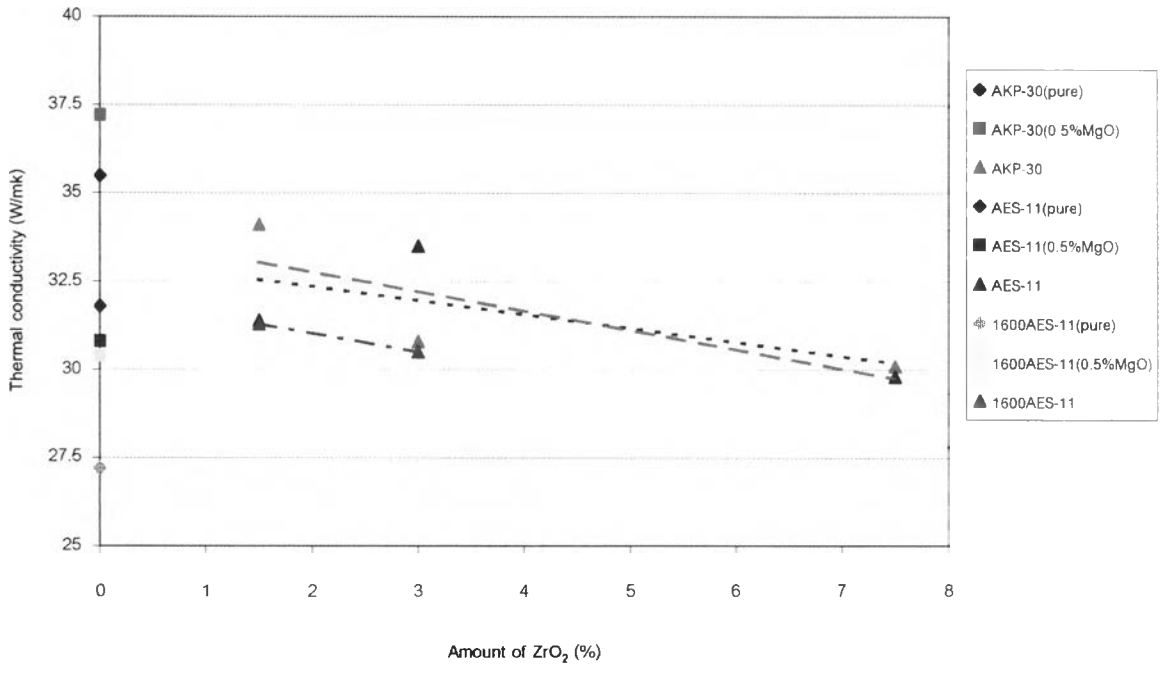

Fig.5.7 Relationship between the amount of ZrO_2 and thermal conductivity of AKP-30 and AES-11.

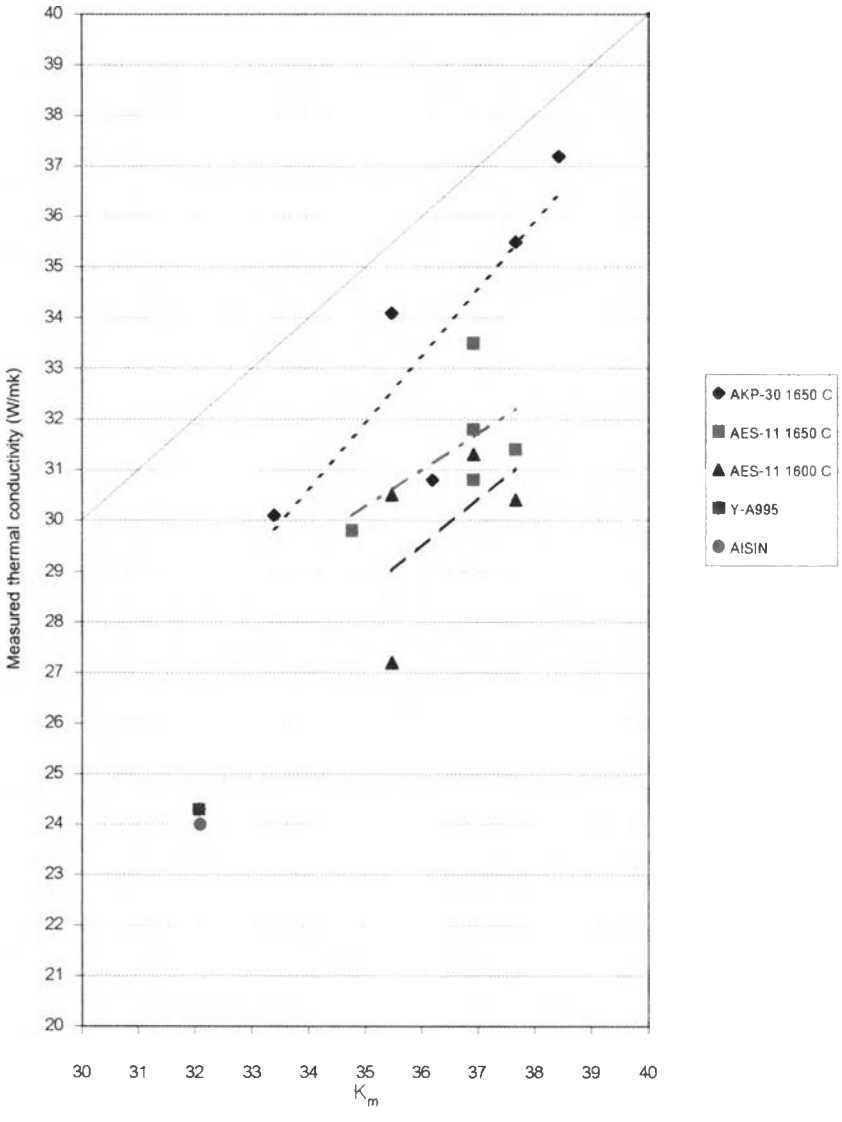

Fig.5.8 Relationship between K_m and measured thermal conductivity (W/m•K).

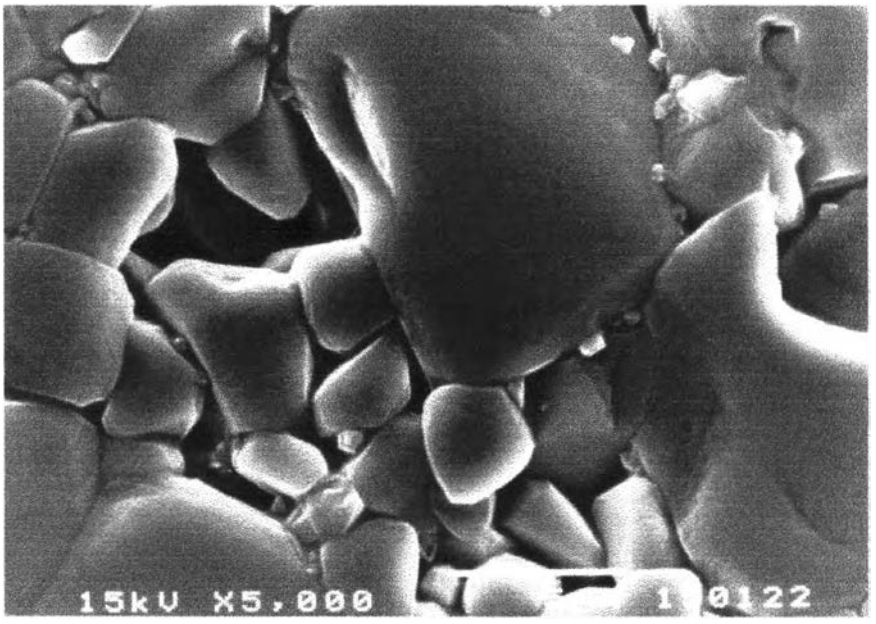

Fig.5.9 SEM micrograph of AISIN substrate.

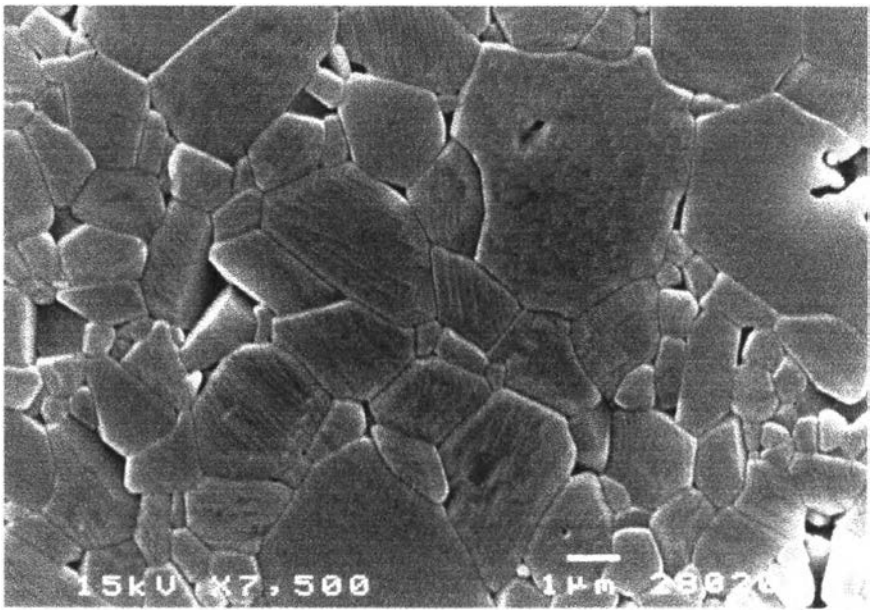

Fig.5.10 SEM micrograph of Y-A995 specimen sintered at 1650 ^{o}C 2 h.